

# IEEE TRANSACTIONS ON GEOSCIENCE AND REMOTE SENSING

A PUBLICATION OF THE IEEE GEOSCIENCE AND REMOTE SENSING SOCIETY



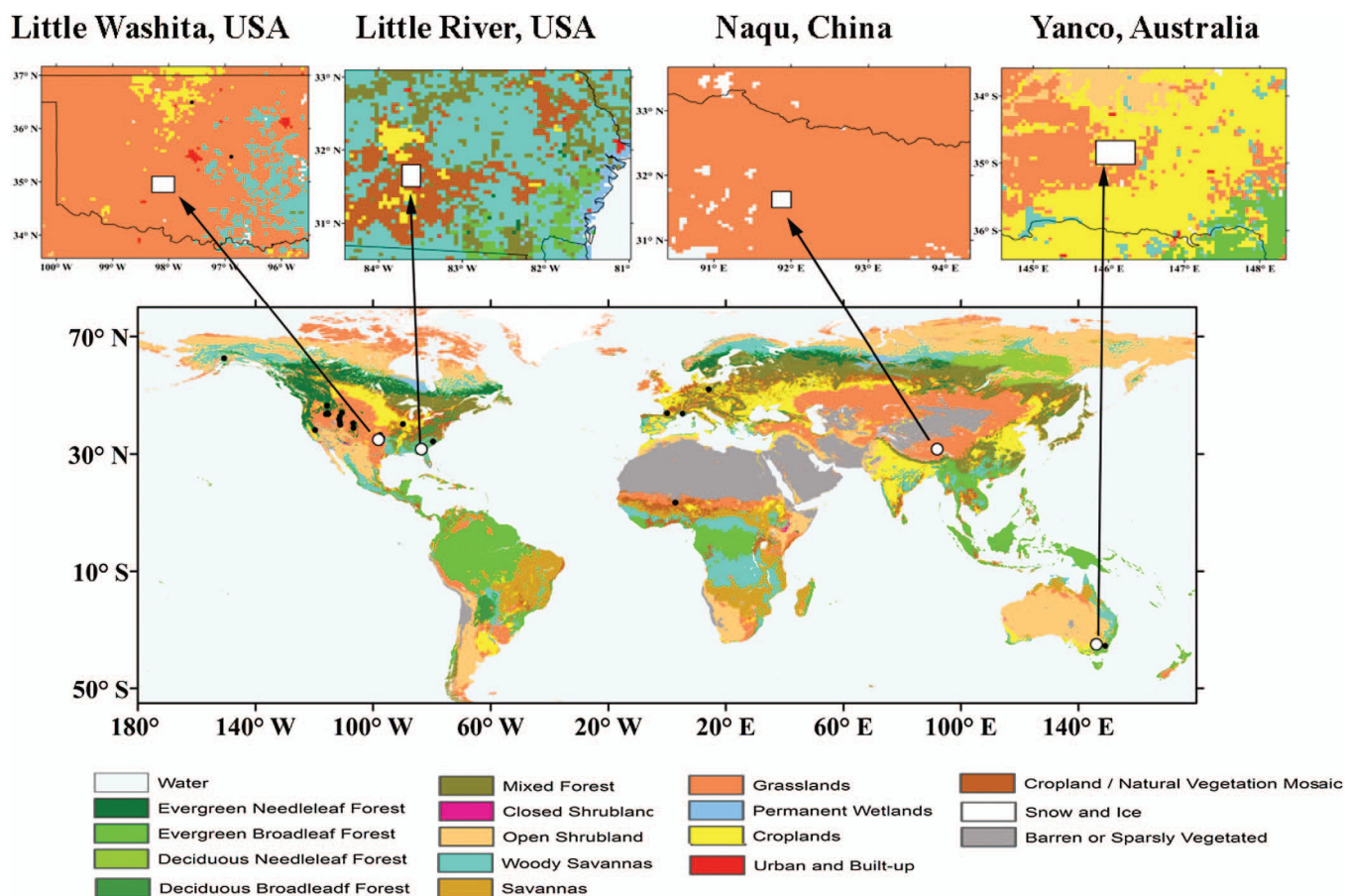
JANUARY 2016

VOLUME 54

NUMBER 1

IGRSD2

(ISSN 0196-2892)



Spatial distribution of the soil moisture network sites used for developing and validating the University of Montana AMSR-E soil moisture retrieval algorithm based on dynamic vegetation scattering properties. Background images represent the MODIS IGBP global land cover map.

# IEEE TRANSACTIONS ON GEOSCIENCE AND REMOTE SENSING

A PUBLICATION OF THE IEEE GEOSCIENCE AND REMOTE SENSING SOCIETY



JANUARY 2016

VOLUME 54

NUMBER 1

IGRSD2

(ISSN 0196-2892)

---

PAPERS

**Atmosphere**

- The Normalized Differential Spectral Sensitivity Approach Applied to the Retrieval of Tropospheric Water Vapor Fields Using a Constellation of Corotating LEO Satellites . . . . . *A. Lapini, F. Cuccoli, F. Argenti, and L. Facheris* 135
- Top-of-Atmosphere Image Simulation in the 4.3- $\mu\text{m}$  Mid-infrared Absorption Bands . . . . . *Y. Liu, W. Zhang, and B. Zhang* 452

**Oceans**

- The Assimilation of Jason-2 Significant Wave Height Data in the North Indian Ocean Using the Ensemble Optimal Interpolation . . . . . *P. Qi and L. Cao* 287
- Spectral Information Adaptation and Synthesis Scheme for Merging Cross-Mission Ocean Color Reflectance Observations From MODIS and VIIRS. . . . . *K. Bai, N.-B. Chang, and C.-F. Chen* 311
- Doppler Simulation and Analysis for 2-D Sea Surfaces Up to Ku-Band. . . . . *J. Wang and X. Xu* 466

**Cryosphere**

- Multiyear Arctic Sea Ice Classification Using OSCAT and QuikSCAT. . . . . *D. B. Lindell and D. G. Long* 167

**Vegetation and Land**

- Microwave Unmixing With Video Segmentation for Inferring Broadleaf and Needleleaf Brightness Temperatures and Abundances From Mixed Forest Observations . . . . . *L. Gu, K. Zhao, and B. Huang* 279
- Passive Microwave Remote Sensing of Soil Moisture Based on Dynamic Vegetation Scattering Properties for AMSR-E . . . . . *J. Du, J. S. Kimball, and L. A. Jones* 597

**Subsurface and Geology**

- Automated Detection of Reflection Hyperbolas in Complex GPR Images With No *A Priori* Knowledge on the Medium . . . . . *L. Mertens, R. Persico, L. Matera, and S. Lambot* 580

**Electromagnetics**

- Evaluation of Phase Coding to Mitigate Differential Reflectivity Bias in Polarimetric PAR . . . . . *I. R. Ivić and R. J. Doviak* 431
- Numerical Computation of the Electromagnetic Bias in GNSS-R Altimetry . . . . . *A. Ghavidel, D. Schiavulli, and A. Camps* 489

---

(Contents Continued on Page 2)

---

Modeling of Ionospheric Time Delay Using Anisotropic IDW With Jackknife Technique . . . . .	V. S. Srinivas, A. D. Sarma, and H. K. Achanta	513
<b>Hyperspectral Data Processing</b>		
Spectral and Spatial Proximity-Based Manifold Alignment for Multitemporal Hyperspectral Image Classification . . . . .	H. L. Yang and M. M. Crawford	51
A Novel Ranking-Based Clustering Approach for Hyperspectral Band Selection. . . . .	S. Jia, G. Tang, J. Zhu, and Q. Li	88
Total-Variation-Regularized Low-Rank Matrix Factorization for Hyperspectral Image Restoration . . . . .	W. He, H. Zhang, L. Zhang, and H. Shen	176
Efficient Rotation-Scaling-Translation Parameter Estimation Based on the Fractal Image Model . . . . .	M. L. Uss, B. Vozel, V. V. Lukin, and K. Chehdi	197
Unsupervised Hyperspectral Band Selection by Dominant Set Extraction . . . . .	G. Zhu, Y. Huang, J. Lei, Z. Bi, and F. Xu	227
A Multilinear Mixing Model for Nonlinear Spectral Unmixing . . . . .	R. Heylen and P. Scheunders	240
Hierarchical Suppression Method for Hyperspectral Target Detection. . . . .	Z. Zou and Z. Shi	330
Spectral-Spatial Adaptive Sparse Representation for Hyperspectral Image Denoising. . . . .	T. Lu, S. Li, L. Fang, Y. Ma, and J. A. Benediktsson	373
Reweighted Sparse Regression for Hyperspectral Unmixing. . . . .	C. Y. Zheng, H. Li, Q. Wang, and C.L. Philip Chen	479
Unsupervised Band Selection Based on Evolutionary Multiobjective Optimization for Hyperspectral Images . . . . .	M. Gong, M. Zhang, and Y. Yuan	544
<b>Image Processing and Analysis</b>		
Manifold Regression Framework for Characterizing Source Zone Architecture. . . . .	H. Zhang, I. Mendoza-Sanchez, E. L. Miller, and L. M. Abriola	3
Vehicle Detection in High-Resolution Aerial Images via Sparse Representation and Superpixels . . . . .	Z. Chen, C. Wang, C. Wen, X. Teng, Y. Chen, H. Guan, H. Luo, L. Cao, and J. Li	103
A Multitemporal Profile-Based Interpolation Method for Gap Filling Nonstationary Data . . . . .	L. Malambo and C. D. Heatwole	252
A New Geostatistical Solution to Remote Sensing Image Downscaling . . . . .	Q. Wang, W. Shi, P. M. Atkinson, and E. Pardo-Igúzquiza	386
A Novel Automatic Change Detection Method for Urban High-Resolution Remotely Sensed Imagery Based on Multiindex Scene Representation . . . . .	D. Wen, X. Huang, L. Zhang, and J. A. Benediktsson	609
<b>Geo-Information Systems</b>		
Detection and Labeling of Sensitive Areas in Hydrological Cartography Using Vector Statistics . . . . .	E. Quirós, M.-E. Polo, and Á. M. Felicísimo	189
<b>Microwave Radiometry</b>		
Impact of Bias Correction Methods on Estimation of Soil Moisture When Assimilating Active and Passive Microwave Observations . . . . .	A. Monsivais-Huertero, J. Judge, S. Steele-Dunne, and P.-W. Liu	262
Conjugate Gradient Method in Hilbert and Banach Spaces to Enhance the Spatial Resolution of Radiometer Data . . . . .	F. Lenti, F. Nunziata, C. Estatico, and M. Migliaccio	397
SMOS Level-2 Soil Moisture Product Evaluation in Rain-Fed Croplands of the Pampean Region of Argentina . . . . .	R. Niclòs, R. Rivas, V. García-Santos, C. Doña, E. Valor, M. Holzman, M. Bayala, F. Carmona, D. Ocampo, Á. Soldano, M. Thibeault, V. Caselles, and J. M. Sánchez	499
<b>Radar Systems</b>		
Robust CFAR Detector Based on Truncated Statistics in Multiple-Target Situations . . . . .	D. Tao, S. N. Anfinsen, and C. Brekke	117
The NASA High-Altitude Imaging Wind and Rain Airborne Profiler . . . . .	L. Li, G. Heymsfield, J. Carswell, D. H. Schaubert, M. L. McLinden, J. Creticos, M. Perrine, M. Coon, J. I. Cervantes, M. Vega, S. Guimond, L. Tian, and A. Emory	298
<b>Synthetic Aperture Radar</b>		
Geodetic SAR Tomography. . . . .	X. X. Zhu, S. Montazeri, C. Gisinger, R. F. Hanssen, and R. Bamler	18
Forcing Scale Invariance in Multipolarization SAR Change Detection. . . . .	V. Carotenuto, A. De Maio, C. Clemente, J. J. Soraghan, and G. Alfano	36
Wideband Interference Mitigation in High-Resolution Airborne Synthetic Aperture Radar Data . . . . .	M. Tao, F. Zhou, and Z. Zhang	74
Compressive Sensing for Multibaseline Polarimetric SAR Tomography of Forested Areas. . . . .	X. Li, L. Liang, H. Guo, and Y. Huang	153

---



---

Airborne DLSLA 3-D SAR Image Reconstruction by Combination of Polar Formatting and $L_1$ Regularization . . . . .	213
..... X. Peng, W. Tan, W. Hong, C. Jiang, Q. Bao, and Y. Wang	
Inclined Geosynchronous Spaceborne–Airborne Bistatic SAR: Performance Analysis and Mission Design. . . . .	343
..... Z. Sun, J. Wu, J. Pei, Z. Li, Y. Huang, and J. Yang	
Exploiting Polarimetric TerraSAR-X Data for Sea Clutter Characterization . . . . .	358
..... E. Makhóul, C. Lopez-Martínez, and A. Broquetas	
A Probabilistic Approach for InSAR Time-Series Postprocessing . . . . .	421
..... L. Chang and R. F. Hanssen	
Novel Model-Based Method for Identification of Scattering Mechanisms in Polarimetric SAR Data . . . . .	520
..... J. Yin, W. M. Moon, and J. Yang	
Ground Moving Target Indication in SAR Images With Symmetric Doppler Views . . . . .	533
..... G. Lv, Y. Li, G. Wang, and Y. Zhang	
Despeckling of SAR Image Using Generalized Guided Filter With Bayesian Nonlocal Means . . . . .	567
..... W. Ni and X. Gao	

**Satellite Systems**

Using Lunar Observations to Validate Clouds and the Earth’s Radiant Energy System Pointing Accuracy. . . . .	65
..... J. L. Daniels, G. L. Smith, K. J. Priestley, and S. Thomas	
Estimation and Correction of Geolocation Errors in FengYun-3C Microwave Radiation Imager Data . . . . .	407
..... F. Tang, X. Zou, H. Yang, and F. Weng	
Spatial Downscaling of Satellite Soil Moisture Data Using a Vegetation Temperature Condition Index . . . . .	558
..... J. Peng, A. Loew, S. Zhang, J. Wang, and J. Niesel	

---

ANNOUNCEMENTS

Call for Papers—IEEE GEOSCIENCE AND REMOTE SENSING MAGAZINE . . . . .	627
---	-----

---

About the Cover: The cover shows the spatial distribution of the selected (solid black circles) International Soil Moisture Network (ISMN) sites used for developing the revised University of Montana (UMT) AMSR-E soil moisture retrieval algorithm; (solid white circles) independent validation site network locations are also denoted, whereas inset maps show detailed subregions surrounding the (white polygons) four soil moisture validation networks used in this study; background images represent the MODIS IGBP global land cover map. Unlike the major AMSR-E retrieval algorithms that assume fixed scattering albedo values over the globe, the revised UMT algorithm adopts a weighted averaging strategy for soil moisture estimation based on a dynamic selection of albedo values that are empirically determined. The resulting soil moisture retrievals demonstrate more realistic global patterns and seasonal dynamics relative to the baseline UMT soil moisture product. Quantitative analysis of the new approach against *in situ* soil moisture measurements over the four regional networks indicates improved performance over the baseline UMT algorithm. The retrieval strategy is also applicable to other passive microwave sensors, including lower frequency (L-band) observations from the Soil Moisture Active Passive (SMAP) mission. For more information please see “Passive Microwave Remote Sensing of Soil Moisture Based on Dynamic Vegetation Scattering Properties for AMSR-E,” by Du *et al.*, which begins on page 597.